TRANSIENT PLASTICITY IN GEOMECHANICS

D. V. Griffiths
Department of Engineering, University of Manchester, U.K.

ABSTRACT: Analyses of geotechnical problems often make the assumption that the soil is either fully drained or fully undrained. The validity of these assumptions depends to a large extent on the permeability of the soil, the drainage path lengths and the rate at which loads are applied. This paper describes a finite element technique which takes account of transient effects through a Biot analysis, enabling coupling of the pore pressure variations to a nonlinear soil stress-strain law.

1 INTRODUCTION

This paper describes three studies in which collapse of geotechnical systems is reached in a time-dependent manner. A program has been developed which couples Biot's (1941) theory for a fluid saturated elastic medium with a simple elastic-perfectly plastic Mohr-Coulomb model for frictional soil. The technique can retrieve drained and undrained behaviour as special cases of the general transient analysis.

The incremental form of the Biot algorithm is described in the next section together with some comments about the implementation of the algorithm in a finite element program. The examples include expansion of a thick cylinder, passive earth pressure and excavation.

In each case 'loading', be it due to applied loads, displacements or body forces (in the case of the excavation analyses) is applied at variable rates to observe the range of behaviour possible between the limits of the fully drained and fully undrained conditions.

2 INCREMENTAL FORMULATION

The matrix equations describing the Biot formulation have been described elsewhere (see e.g. Smith and Griffiths 1988), however if the equations are to be used in conjunction with a nonlinear constitutive stress-strain law, an incremental formulation becomes essential.

In the present work the element matrix version of the Biot equations in incremental form is presented below:

$$\begin{bmatrix} \mathbf{k_m} & \mathbf{C} \\ \mathbf{C}^T & -\theta \Delta t \mathbf{k_p} \end{bmatrix} \begin{Bmatrix} \Delta \mathbf{r} \\ \Delta \boldsymbol{\phi} \end{Bmatrix} = \begin{Bmatrix} \Delta \mathbf{f} \\ \Delta t \mathbf{k_p} \boldsymbol{\phi}_o \end{Bmatrix} \tag{1}$$

where

$\mathbf{k_m}$	element solid stiffness matrix	$\mathbf{k_p}$	element fluid stiffness matrix
$\mathbf{C}$	element coupling matrix*	$\Delta \mathbf{r}$	change in nodal displacements
$\Delta \boldsymbol{\phi}$	change in nodal excess pore-pressures	$\boldsymbol{\phi}_o$	'old' excess pore-pressures
$\Delta \mathbf{f}$	change in nodal forces	Δt	calculation time step
θ	time stepping parameter (= 1)		

This is similar to the formulation reported by Sandhu (1981) and used by Hicks (1990) and Griffiths *et al* (1991) .

When the incremental equations (1) are implemented in a finite element code, the global version of the same equations are formed following assembly of the solid and fluid matrices, $\mathbf{k_m}$ and $\mathbf{k_p}$ respectively into their global counterparts. The right-hand-side vector must also be formed from the incremental nodal forces and the product of the fluid matrix and the pore pressures from the previous increment.

It should be noted that the global 'stiffness' matrix will have negative terms on its main diagonal due to the $-\Delta t\theta\mathbf{k_p}$ terms. It will therefore not be possible to use a conventional Cholesky split approach which needs to take square roots of the diagonal terms. A conventional Gaussian elimination approach is recommended together with a 'skyline' strategy for storage.

Another point refers to the product $\mathbf{k_p}\phi_o$ which appears on the right-hand-side. This contribution to the global 'force' vector is conveniently formed using *element-by-element* products. This avoids the need to declare a secondary 'force' vector at the global level relating to this particular product.

3 THICK WALLED CYLINDER

The analysis is of a thick-walled cylinder of saturated soil in plane strain subjected to an internal pressure which increases linearly with time. The problem is to estimate the ultimate internal pressure that the cylinder can sustain as a function of the *rate* of loading. Results for this type of problem were first reported by Small *et al* (1976).

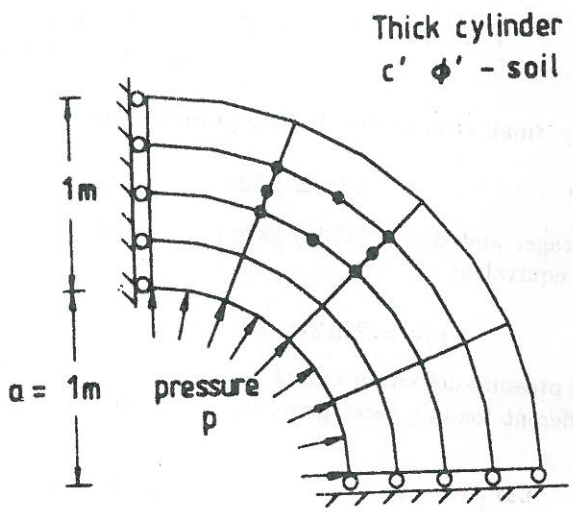

Figure 1 Mesh used for thick cylinder analysis.

A typical finite element mesh is shown in Figure 1 for a cylinder in which the outer radius is twice the inner radius. The mesh consists of 8-node elements for the solid phase and 4-node elements for the fluid phase (Zienkiewicz 1977). Four Gauss- points per element were used for all integration.

The soil was initially stress-free and given the following effective properties:

$$\begin{array}{llll} E' = 200\ \text{kPa} & \nu' = 0 \\ \phi' = 30^\circ & c' = 1\ \text{kPa} \\ \psi' = 0 & k/\gamma_w = 1\ \text{m}^4/(\text{kNs}) \end{array}$$

A dimensionless time factor is introduced, given by:

$$T_v = \frac{c_v t}{a^2} \tag{2}$$

where a is the internal radius of the cylinder (in this case equal to unity), and t represents time.

The coefficient of consolidation c_v is defined:

$$c_v = \frac{k(1-\nu')E'}{\gamma_w(1-2\nu')(1+\nu')} \tag{3}$$

Thus $c_v = 200\text{m}^2/\text{s}$ in this case.

The rate of increase of internal pressure acting on the cylinder is expressed in the following non-dimensional form:

$$\omega = \frac{d(p/c')}{T_v} \tag{4}$$

where p is the time dependent internal pressure on the cylinder.

The behaviour of the soil during 'fast' loading approximates to undrained conditions. With the dilation angle equal to zero, no volume change will occur during shear and the mean effective stress will remain constant and equal to zero during loading. For the undrained case, the following soil 'properties' will operate:

$$E_u = 1.5E'/(1+\nu') = 300\text{kPa} \qquad \nu_u \approx 0.5$$
$$\phi_u = 0 \qquad c_u = c'\cos\phi'$$

The failure load quoted by Small *et al* for the drained problem was:

$$p/c' = 1.02 \tag{5}$$

In the undrained case, Prager and Hodge (1968) gave $p/c_u = 2\ln 2$, which for a Mohr-Coulomb material with $\phi' = 30^o$ is equivalent to:

$$p/c' = 2\ln 2\cos 30^o = 1.20 \tag{6}$$

The non-dimensionalised pressure-deflection curves computed using the present method are given in Figure 2 for three different loading rates given by $\omega = 16$ (fast), $\omega = 4$ (intermediate) and $\omega = 0.1$ (slow).

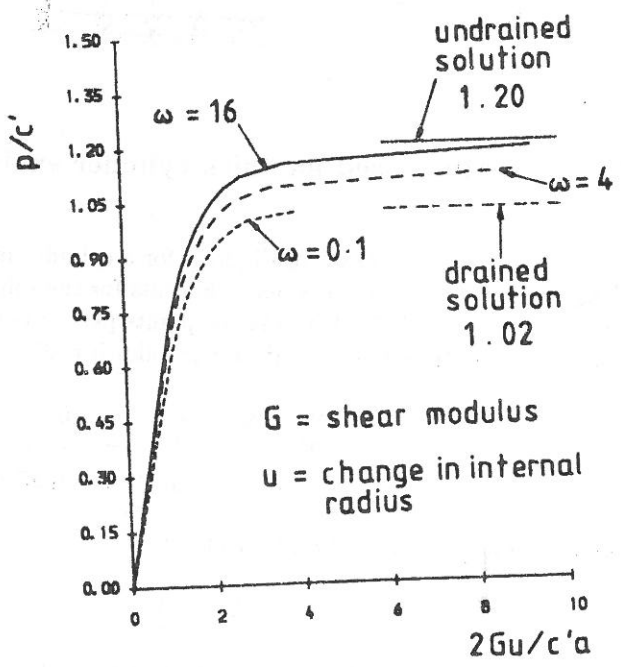

Figure 2 Stress vs. Displacement for different loading rates.

4 PASSIVE EARTH PRESSURE

The transient analyses were next applied to a problem of passive earth pressure. The practical applications of such a study relate to the dredging process, whereby underwater soils are removed by excavators in order to maintain sufficient depth in ports, harbours, rivers and canals.

In this section, the effect of wall speed on passive resistance of non-dilative soils is considered. The plane strain mesh geometry is shown in Figure 3. The simple boundaries of the problem (see e.g. Crisfield 1987), removes the shear concentration that would normally be observed at the base of the wall, but does not detract from the analysis in the case of a smooth wall .

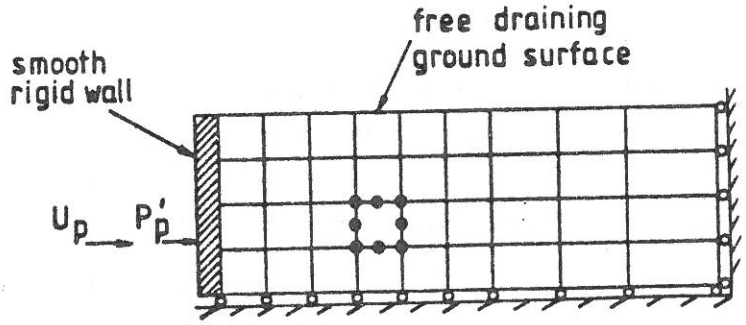

Figure 3 Mesh for passive earth pressure analysis.

The excavation blade is idealised as a rigid vertical smooth wall translated horizontally into the soil bed. All boundaries of the mesh are impermeable except the top surface at which drainage can occur.

The soil is given the following properties:

E'	=	1×10^4 kPa	ν'	=	0.25
c'	=	0 kPa	ϕ'	=	$30°, (K_p = 3)$
ψ'	=	0	γ'	=	10 kN/m^3
K_o	=	0.5	k/γ_w	=	1×10^{-5} m^4/(kN.s)
c_v	=	0.12 m^2/s			

where γ' is the submerged unit weight and K_o is the coefficient of earth pressure at rest. The wall height equals 1 metre.

A dimensionless dredging rate L_R is used to represent the (constant) speed of the wall as it moves into the soil. This quantity is defined:

$$L_R = \frac{d(x/H)}{dT_d} \tag{7}$$

with the time factor T_d given by:

$$T_d = \frac{c_v t}{H^2} \tag{8}$$

The height of the wall is H, and x represents the distance moved by the wall after time t. The effective soil force P'_p against the wall was computed by integrating the horizontal effective stresses in the column of elements adjacent to the wall. These forces are plotted in dimensionless form in Figure 4 for three rates of wall displacement. In each case, the total wall displacement was achieved numerically using 60 equal increments. The calculation time step was 0.001, 0.1 and 10 seconds respectively for the 'fast', 'intermediate' and 'slow' cases.

At the fast dredging rate ($L_R = 1.0$), the soil behind the wall behaves in an undrained manner, whereas at the slow dredging rate ($L_R = 0.0001$), drained conditions are approximated. An intermediate response is observed at the compromise dredging rate ($L_R = 0.01$).

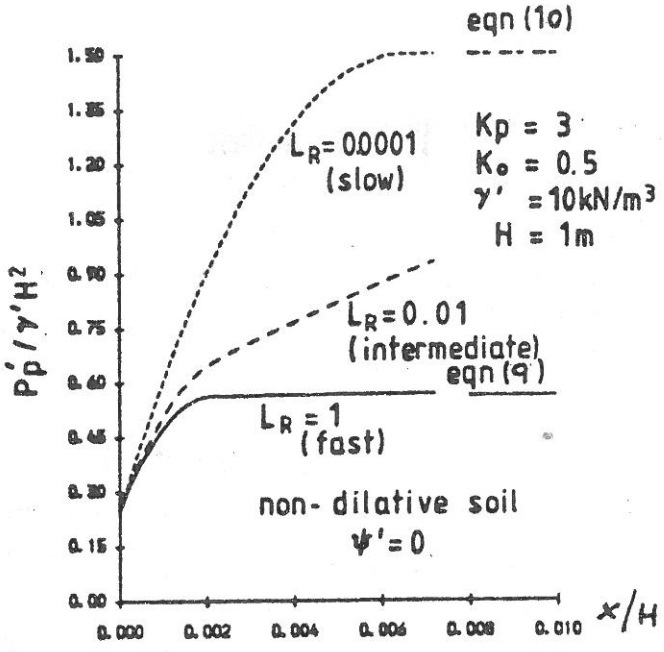

Figure 4 Force vs Displacement for different displacement rates.

In the undrained case, the analytical solution (Griffiths 1985, Li 1988) for the effective passive force is given by :

$$P_p' = \frac{1}{2}\gamma' H^2 \frac{K_p(K_o+1)}{K_p+1} \tag{9}$$

In the drained case, the simple Rankine solution is obtained:

$$P_p' = \frac{1}{2}\gamma' H^2 K_p \tag{10}$$

The computed values in Figure 4 are seen to agree closely with equations (9) and (10).

As the soil model used in these analyses was non-dilative, the slow moving wall (drained) led to greater passive resistance than the fast moving wall (undrained) in which compressive pore pressures were generated in the elastic phase of the stress-strain behaviour.

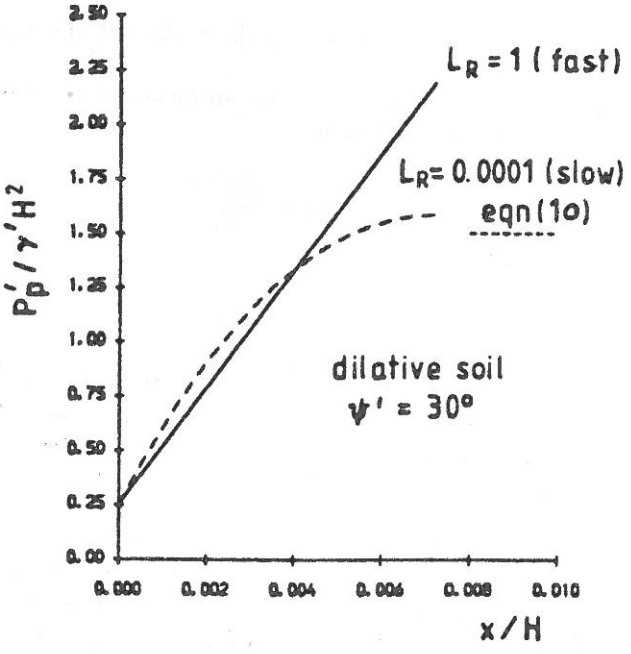

Figure 5 Force vs Displacement for different dilation angles.

Figure 5 shows the effect of the dilation angle on the effective force behind the wall for the 'fast' and 'slow' cases. In the 'fast' case, the effective force continues to rise well past the drained Rankine solution. In the 'slow' case, the dilation angle makes virtually no difference to the solution, and the result converges on the drained solution given by equation 10.

In the present work, the dilation angle is constant and this is a deficiency of the simple model. In 'real' soils, continuous shearing will reduce the rate of dilation until the critical state is reached, at which point soil continues to shear at constant volume and constant pore pressure (see e.g. Seed and Lee 1967) .

5 EXCAVATION

This section describes some analysis in which the stability of a vertical cutting in a saturated c', ϕ' soil is shown to be affected by the *rate* of excavation.

The excavation was simulated by the removal of horizontal rows of elements in the mesh. Forces generated by this action were applied to the new mesh boundary. The boundary forces at the i^{th} stage of an excavation are given by:

$$F_i = \int_{V_i} B^T \sigma_{i-1} dV - \int_{V_i} N^T \gamma dV \qquad (11)$$

The first term in (11) is the nodal internal resisting force vector due to the stresses that existed in the removed elements, and the second term represents the reversal of the nodal body-forces of those elements assuming that γ is acting in the negative direction (see e.g. Ghaboussi and Pecknold 1984 , Holt 1991).

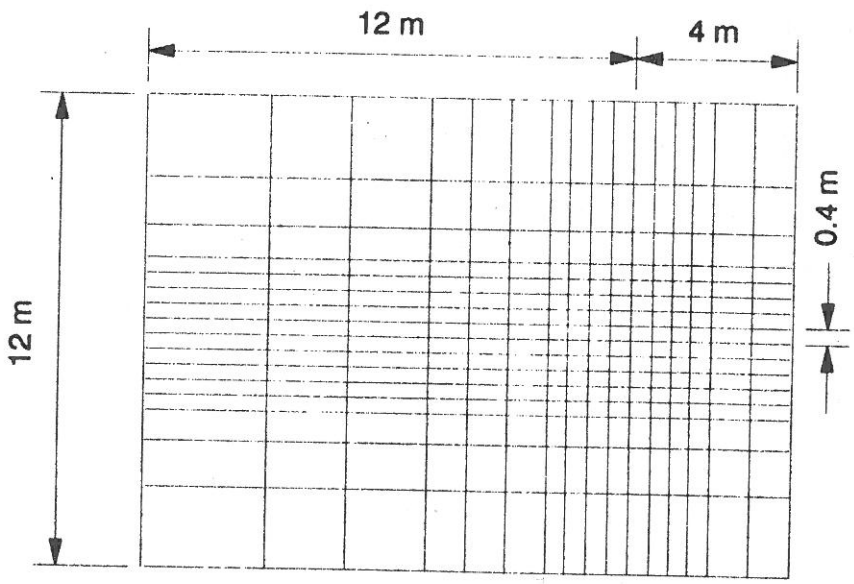

Figure 6 Mesh for excavation analysis.

Figure 6 shows a typical finite element mesh for the excavation analyses. The analysis is in plane strain so the mesh will represent half the eventual excavation. The soil properties are given in the table below.

E'	=	1.0 x 10^5 kPa	ψ'	=	0.0°
ν'	=	0.43	γ'	=	20.0 kN/m^3
ϕ'	=	15°	K_o	=	0.75
c'	=	16°	k/γ_w	=	1.0 m^4/(kN.s)

For the given values of c' and ϕ', the drained critical depth from Taylor's (1948) charts is 4.0m. Excavation of a 4m wide strip was carried out 'slowly' until failure occurred. The computed result indicated a critical depth at 4.4m, some 9.1% higher than Taylor's value. The difference was thought to be due to the rather crude mesh of Figure 6 in which each excavation was limited to a minimum of 0.4m.

The previous result was obtained with a 'slow' excavation leading to a drained solution. In order to investigate rate-effects on excavation stability, the next set of results were obtained by keeping a constant excavation rate of 1 m/s but systematically reducing the permeability coefficient K ($= k/\gamma_w$) by an order of magnitude at a time in the range:

$$1.0 \times 10^{-10} \leq K_{x,y} \leq 1.0 \times 10^{-1} \qquad \text{m}^4/(\text{kN.s}) \tag{12}$$

As the permeability was reduced, the excavation tended towards a 'fast' rate and hence an undrained solution.

It was found that the lower the permeability of the soil the higher the value of the critical depth obtained due to the retention of the pore fluid following unloading effects during excavation. The upper limit of the critical depth corresponding to undrained conditions was found to be 5.6m for values of the permeability coefficient of 1.0×10^{-7} m^4/(kN.s) or less.

To investigate more closely the transient region between the upper and lower limits ('drained' or 'undrained'), a considerably finer mesh was employed together with a smaller step size on the permeability coefficient (Holt 1991). As shown in Figure 7, the upper limit for the critical depth was unchanged at 5.6m, however the lower limit was reduced to 4.2m, now less than 5% in 'error' with Taylor's analytical solution.

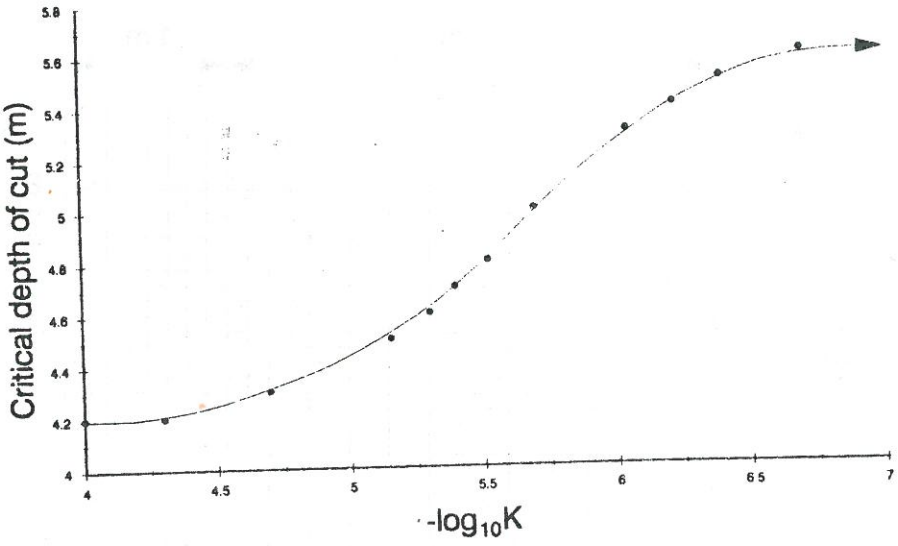

Figure 7 Critical height vs. permeability

6 CONCLUDING REMARKS

The paper has described three examples of transient analysis in geomechanics in which the strength of a saturated soil mass has depended on the *rate* of loading. The algorithm involved combining an *incremental* version of Biot's equations for a porous elastic medium with a simple elastic-perfectly plastic Mohr-Coulomb constitutive law. In all cases, the drained and undrained limits were retrieved as special cases of the transient analysis and comparison made with analytical solutions when available.

It should be emphasised that the results presented herein were based on a simple elasto-plastic soil model which assumed no plastic volume change at failure. The resulting undrained stress

paths approximate to 'medium' dense materials; however if the soil under investigation exhibited significant dilative or contractive tendencies, the 'simple' model would not be suitable and a more sophisticated soil model would be required. Of particular interest would be a soil which exhibited contractive tendencies during shear. Such a material could experience a rapid loss of strength during undrained loading. In the context of excavation analysis for example, this kind of behaviour might lead to the undrained case being *more* critical than the drained case. Such behaviour was indicated in examples of slope stability by Hicks and Wong (1988) , and studies are continuing at Manchester University in this area.

REFERENCES

[1] M.A. Biot. General theory of three-dimensional consolidation. *Journal of Applied Physics*, 12:155–164, 1941.

[2] M.A. Crisfield. Plasticity computations using the Mohr-Coulomb yield criterion. *Engineering Computations*, 4(4):300–308, 1987.

[3] J. Ghaboussi and D.A. Pecknold. Incremental finite element analysis of geometrically altered structures. *International Journal for Numerical Methods in Engineering*, 20:2151–2164, 1984.

[4] D.V. Griffiths, M.A. Hicks, and C.O.Li. Transient passive earth pressure analyses. *Géotechnique*, 41(4):615–620, 1991.

[5] M.A. Hicks. *Numerically modelling the stress-strain behaviour of soils.* PhD thesis, Department of Engineering, University of Manchester, 1990.

[6] M.A. Hicks and S.W. Wong. Static liquefaction of loose slopes. In G. Swoboda, editor, *Proceedings of the 6th International Conference on Numerical Methods in Geomechanics*, pages 1361–1368. A.A. Balkema, Rotterdam, 1988.

[7] D.A. Holt. Transient analysis of excavations in soil. Master's thesis, Department of Engineering, University of Manchester, 1991.

[8] R.S. Sandhu. Finite element analysis of coupled deformation and fluid flow in porous media. In J.B. Martins, editor, *Numerical Methods in Geomechanics*, pages 203–228. D. Reidel Publishing Company, Dordrecht, Holland, 1981.

[9] H.B. Seed and K.L. Lee. Undrained strength characteristics of cohesionless soils. *Journal of the Soil Mechanics and Foundation Engineering Division, ASCE*, 93(SM6):333–360, 1967.

[10] I.M. Smith and D.V. Griffiths. *Programming the Finite Element Method.* John Wiley and Sons, Chichester, New York, 2nd edition, 1988.

[11] D.W. Taylor. *Fundamentals of soil mechanics.* John Wiley and Sons, Chichester, New York, 1948.